International Journal for Multidisciplinary Research (IJFMR)
E-ISSN: 2582-2160 ● Website: www.ijfmr.com ● Email: editor@ijfmr.com

# UV-Visible, FT-IR, FT-Raman, NMR Spectra, Molecular Structure, ESP and HOMO–LUMO Investigation of Coumarin Derivative

**Mayadevi Kalgi[1], Shivaleela B[2], Mahantesh B[3], Tipperudrappa J[4], S M Hanagodimath[5]**

[1]Department of Physics, Nrupatunga University (Formerly Government Science College), Bangalore-560001, Karnataka, India
[2,5]Department of Physics, Gulbarga University, Kalaburagi-585106, India
[3]Department of Chemistry, P.C. Jabin Science College, Hubli-580031, Karnataka, India
[4]Department of Physics, Vijayanagar Sri Krishnadevaraya University, Ballari-583105, Karnataka, India

**Abstract**
Computational studies on biologically active coumarin derivatives have been studied using Gaussian 16 software. Coumarin molecule with the substitution of benzene and methoxy group Viz., 4IPBC have been used to carry the quantum chemical calculations. Parameters like absorption maxima, oscillator strength and excited state energies, are obtained from UV-Visible absorption maxima. Semi-empirical method is the convenient tool to study optimized geometry. Spectroscopic analysis of NMR, IR and Raman spectra have been studied using DFT method at 6-311++G(d, p)/B3LYP basis set. The ground state dipole moments are smaller than the excited state dipole moment determined by TD-DFT technique. The use of IR and Raman vibrational bands facilitates the study of the bending and stretching modes of vibration in the molecule. $H^1$ and $C^{13}$ NMR shielding values were evaluated from NMR spectra using GIAO method. HOMO-LUMO, MESP map and Mulliken atomic charges give charge distribution within the molecule.

**Keywords:** Coumarin derivatives, TD-DFT, GIAO, Mulliken charges, Molecular orbital

## 1. Introduction

Coumarins are well known laser dyes for the blue-green spectral region. They exhibit a strong fluorescence in UV-Visible region. As consequence, they work better as dye laser media, colorants and NLO chromospheres. Coumarins are fluorescent probes used in medicine to measure the fluidity and stiffness of living cells and their surrounding media. Additionally, they have unique biological qualities that include fungicidal, anticoagulant, antibacterial, antimicrobial, analgesic, anti-pyretic, anticancer, and antimetastatic effects[1]. These compounds are used as rodenticides, high-performance liquid chromatography, fluorescence probes for protein studies, fluorescent ionophoresfluorescent indicators, optical brighteners and laser dyes in the blue-green region[2-9].

Coumarin moiety as such is non-fluorescent, however, coumarins having substituent at different places show fluorescence[10]. The type of substituent, its location on the coumarinring, and its surroundings all

significantly affect the spectrum properties of these coumarin dyes. The substitution modifies the location of the absorption and fluorescence bands, the excited state dipole moment of the substituted coumarin molecule, and its solubility in organic solvents. In some environments, it also affects the molecule's resistance to chemical and photochemical protonation.In this present work we used two benzocoumarin derivative 4-(2-iodo phenoxymethyl)-benzo[f]chromen-3-one(4IPBC) [11,12]. Present paper reports the effect of solvent and substituent on these, 4IPBC coumarin molecules having almost identical structure with different substituentLiterature reports that 4-aryloxymethyl coumarins have centrosymmetric nature, long range coupling, and antibacterial action. Recently synthesized 4-aryloxymethyl coumarins have been found to have improved anti-mycobacterial and anti-cancer properties.

As there has never been a study of this kind on any molecule to the best of our knowledge, computational research on biomolecules has already arisen as a theoretical way to predict its qualitative structure property relationship. The computational study on spectroscopic characteristics like IR active vibrations & Raman activity[13], electronic transitions in UV-Vis spectra, $^{1}H$ &$^{13}C$ NMR chemical shifts[14], thermo chemistry, nonlinear optical properties and chemical reactivity descriptors has been carried out using Density functional theory (DFT) with B3LYP functional and 6-311++G(d, p) basis set; DFT predicts structural properties, lowest energy of the probe in gas phase and in the solvent[15,16]. Chemical reactivity analysis has been carried out to investigate the physical principle applicable to elucidate its bioactivity[17].

The aim of the present work is to study spectral behaviour of 4-aryloxymethyl coumarins from quantum chemical calculations. The investigation of photophysical properties of ground and excited state dipole moments, vibrational modes, chemical shifts, atomic charges and molecular orbital of organic molecules has been a major area of discussion. Furthermore, computational value of ground and singlet excited state dipole moments are calculated by density functional theory (DFT)and time dependent density functional (TD-DFT) level of theory in various solvents.Similarly, DFT method also has been used to predict vibrational modes from IR-Raman spectra and Chemical shifts from NMR Spectra. Charge transfer within the molecule was correlated by Mulliken atomic charges, contour map and molecular electrostatic potential (MEP) map.

## 2. Computational methods

The coumarin derivatives that have been used for the present computational studyare shown in **Fig. 1**. Various molecular properties have been studied for optimized geometry using Gaussian 16W[18]. UV-Visible spectra of molecules have been obtained for the optimized geometry in Methanol using computational methods such as TD-DFT (Time-Dependent Density Functional Theory). Effect of solvent in TD-DFT method analysed using IEFPCM (Integral Equation Formalism Polarizable Continuum Model). Evaluation of IR (Infrared) and Raman activity were carried out using DFT method at 6-311++G(d, p)/B3LYP basis set for optimized geometry from HF method. Similarly, NMR (Nuclear Magnetic Resonance) shielding values were studied using well known GIAO (Gauge Independent Atomic Orbital) approach. Mulliken atomic charges, Highest Occupied Molecular Orbital (HOMO) and Lowest Unoccupied Molecular Orbital (LUMO),counter map and Electrostatic map (ESP)have been extracted for TD-DFT method[19].

## 3. Results and discussion

Optimized geometry of the probe was obtained using Semi-empirical method with PM6 basis set via Gaussian 16 software. The structure of molecule optimized using three different methods viz., Semi-empirical method. Optimized geometries are shown in **Fig. 1**, whereas arrow mark indicates the direction of dipole moment.Theoretically calculated ground state dipole moment was found to be 7.151 D from Semi-empirical method and 7.770 D, for HF method for four molecules[20,21].

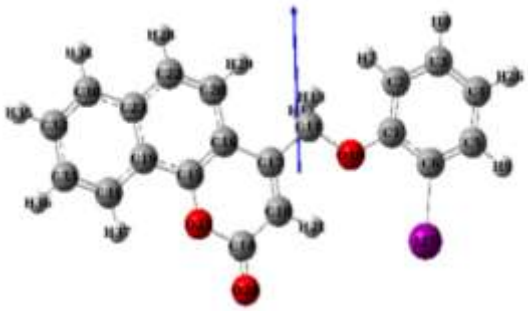

**Fig. 1 Optimized geometry of 4IPBC dipole moment vector.**

### 3.1 UV-Visible spectra

The three excited state energies have been given for respective transition. Absorption maxima for lower-lying singlet states of the molecule have been calculated by TD-DFT 6-311++G(d, p) method. The computed properties such as absorption wavelength, excitation energies (E) and oscillator strengths (f) are listed in **Table 1**. Theoretical UV-Vis spectra of molecule in different solvents are shown in **Fig. 2**. The wavelength at which maximum absorption occurs is associated with the electronic shift from HOMO to LUMO.This transition (H-L) confirms the transition[22]. Oscillator strength is a dimensionless quantity that describes the strength of an electronic transition. If oscillator strength is maximum there is possibility of presence of UV-Visible spectra and if minimum will have less absorption coefficient, if it is zero then the transition is not at all possible[23].

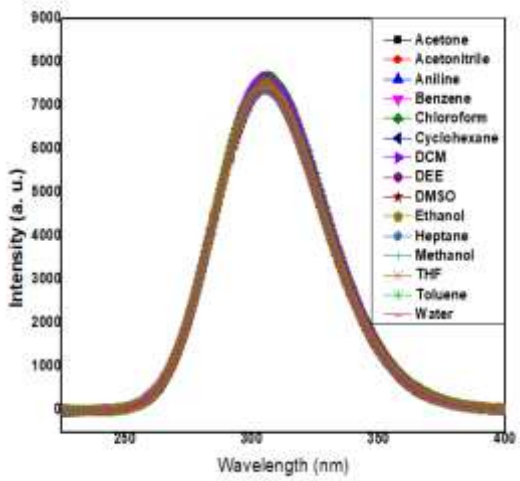


**Fig.2 UV-Vis spectra of 4IPBC in different solvents.**

UV-Visible spectra obtained using TD-DFT methods, in different solvents are shown in **Figs. 2.** The three values of absorption maxima ( $\lambda_1$, $\lambda_2$ and $\lambda_3$), oscillator strength ( $f_1$, $f_2$ and $f_3$) and excited

state energies ( $E_1$, $E_2$ and $E_3$) of the molecules are given in **Tables 1.** For 4IPBC absorption maxima in various solvents is 305 nm, 303 nm and 292 nm, corresponding to excited state energies are 4.060 eV, 4.079 eV and 4.235 eV respectively for oscillator strength 0.1824, 0.003 and 0.0010, are given in **Table 1**.

**Table 1 Absorption maxima, oscillator strength and excited state energy (eV) of 4IPBC using TD-DFT method in different solvents.**

| **Solvents** | **Absorption** | | | **Oscillator strength** | | | **Energy** | | |
|---|---|---|---|---|---|---|---|---|---|
| | $\lambda_1$ | $\lambda_2$ | $\lambda_3$ | $f_1$ | $f_2$ | $f_3$ | $E_1$ | $E_2$ | $E_3$ |
| Acetone | 305 | 303 | 292 | 0.1824 | 0.0003 | 0.0010 | 4.060 | 4.079 | 4.235 |
| AN | 305 | 303 | 293 | 0.1813 | 0.0003 | 0.0010 | 4.061 | 4.084 | 4.228 |
| Benzene | 305 | 303 | 285 | 0.0003 | 0.1916 | 0.0010 | 4.007 | 4.045 | 4.341 |
| CH | 305 | 303 | 284 | 0.0003 | 0.1868 | 0.0010 | 3.999 | 4.048 | 4.353 |
| DCM | 305 | 303 | 291 | 0.1869 | 0.0004 | 0.0010 | 4.055 | 4.065 | 4.256 |
| DEE | 305 | 303 | 288 | 0.0003 | 0.1820 | 0.0010 | 4.041 | 4.057 | 4.293 |
| DMSO | 305 | 303 | 293 | 0.1864 | 0.0003 | 0.0010 | 4.057 | 4.086 | 4.225 |
| Ethanol | 305 | 303 | 292 | 0.1825 | 0.0003 | 0.0010 | 4.060 | 4.081 | 4.232 |
| Heptane | 305 | 303 | 284 | 0.0003 | 0.1842 | 0.0010 | 3.995 | 4.050 | 4.258 |
| Methanol | 305 | 303 | 293 | 0.1801 | 0.0003 | 0.0010 | 4.062 | 4.084 | 4.229 |
| THF | 305 | 303 | 290 | 0.1852 | 0.0008 | 0.0010 | 4.055 | 4.060 | 4.263 |
| Toluene | 305 | 303 | 285 | 0.0003 | 0.1913 | 0.0010 | 4.010 | 4.045 | 4.337 |
| Water | 305 | 303 | 293 | 0.1805 | 0.0003 | 0.0010 | 4.062 | 4.088 | 4.222 |
| Aniline | 306 | 305 | 290 | 0.1965 | 0.0003 | 0.0010 | 4.046 | 4.058 | 4.266 |
| chloroform | 306 | 305 | 289 | 0.0006 | 0.1881 | 0.0010 | 4.045 | 4.052 | 4.286 |

Due to variations in the electron concentrations in the ground and excited states, molecules have distinct dipole moments in each of these states. Therefore, a methodical examination of the solvent effect is instructive and useful for examining the behavior of the molecule in its excited state[24]. Understanding the dipole moment gives information about the electron density and charge distribution surrounding the molecule. DFT was used to compute the ground state dipole moment, and the TD-DFT formalism was used to determine the excited state energies.Ground state ( $\mu_g$ ), excited state ( $\mu_e$ ) and change in dipole moment ($\Delta\mu$) are given in **Table 2**. The $\mu_g$ values obtained from DFT method at 6-311++G(d, p)/B3LYP method for different solvents is around 5.492 D for and 4IPBC respectively. It can be observed from this table, that ICT confirms the $\pi \rightarrow \pi^*$ transition. Ground state dipole moment is smaller than the excited state dipole moment. This statement indicates that a larger charge transfer could take place in excited state than in ground state and also a large dipole moment in excited state than in ground state[25]. Experimental data on excited states are also useful in the parameterisation of quantum chemical methods[26].

**Table 2 Ground state, excited state and change in dipole moment (Debye) of the molecules.**

| | **4IPBC** |
|---|---|

| **Solvents** | $\mu_g$ | $\mu_e$ | $\Delta\mu$ |
|---|---|---|---|
| Acetone | 5.492 | 7.545 | 2.053 |
| Acetonitrile | 5.533 | 7.602 | 2.069 |
| Aniline | 5.318 | 7.304 | 1.986 |
| Benzene | 4.908 | 6.735 | 1.827 |
| Chloroform | 5.211 | 7.155 | 1.944 |
| Cyclohexane | 4.845 | 6.648 | 1.803 |
| DCM | 5.375 | 7.383 | 2.008 |
| DEE | 5.175 | 7.106 | 1.931 |
| DMSO | 5.546 | 7.621 | 2.075 |
| Ethanol | 5.509 | 7.568 | 2.059 |
| Heptane | 4.816 | 6.607 | 1.791 |
| Methanol | 5.528 | 7.595 | 2.067 |
| THF | 5.336 | 7.328 | 1.992 |
| Toluene | 4.93 | 6.766 | 1.836 |
| Water | 5.564 | 7.645 | 2.081 |

### 3.2 IR and Raman Spectra

Finding vibrational modes associated with the compound's estimated particular molecular structure is the goal of the vibrational analysis. Any molecule will have (3N-6) vibrational modes.Whereas N is the number of atoms present in the molecule with three rotational degrees of freedom. There are 37 atoms and 105 vibrational modes of frequency for and 4IPBC. The vibrational band assignments of molecules have been made by using Gauss View molecular visualization program. FT-IR and FT-Raman frequencies for various modes of vibrations are presented in **Table 3**. The experimental Infrared and Raman spectra in gas phase were shown in **Fig. 3 (a and b)** along with calculated FT-IR and FT-Raman spectra, we have presented the calculated vibrational wavenumbers. Generally the high vibrational wavenumbers are characteristic stretching vibrations associated with the functional groups of a molecule.There are different type of bonds C-I, C=C, C-H, C=O and $CH_3$, C-H stretching vibrations are sensitive to hydrogen bonding[27].

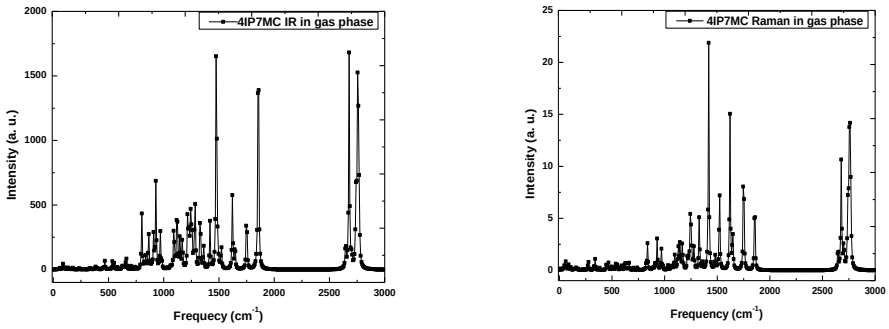


(a) (b)

**Fig. 3 IR and Raman spectra of the molecules in gas phase.**

For 4IPBC, a strong band locating at C-H stretching mode gives peak at 2764 $cm^{-1}$ as seen from **Fig 3a.**FT-IR spectrum is attributed to the C-Hstretching vibrations at 2681 $cm^{-1}$.Usually the C-H vibrations

have been observed between 2500 $cm^{-1}$ to 3000$cm^{-1}$. The band located at 1645 $cm^{-1}$ in the FT-IR spectrum band has been designated as C=C stretching mode. The theoretical band at 1477 $cm^{-1}$ is associated with C=C and C-H stretching mode, which is combined with ring torsion mode. Wavenumbers 857 $cm^{-1}$ corresponds to $CH_2$stretching mode in the molecule. For FT-Raman **Fig 3b** 2759 $cm^{-1}$ C-H stretching mode has been observed, 1732 $cm^{-1}$corresponds to C=C stretching mode. The vibrational modes observed at 1512 $cm^{-1}$for 1477 $cm^{-1}$and 1412 $cm^{-1}$ related to both C=C stretching and C-H bending [28].

**Table 3 IR and Raman maximum vibrational modes of fluorophore in vacuum.**

| **Molecule** | **IR** | | **Raman** | |
|---|---|---|---|---|
| | Frequency ($cm^{-1}$) | Vibrational modes | Frequency ($cm^{-1}$) | Vibrational modes |
| 4IPMC | 857 | $CH_2$ Bending | 1412 | C=C Stretching C-H Bending |
| | 1477 | C=C Bending C-H Stretching | 1477 | C=C Stretching C-H Bending |
| | 1645 | C=C Stretching | 1512 | C=C Stretching C-H Bending |
| | | | | |

### 3.3 NMR Spectra

NMR provides distortions or broad resonance peaks for non-carbon protons. Highly accurate values can be produced if the molecule is small[29]. The GIAO method was one of the most common approaches for calculating isotropic nuclear magnetic shielding tensors. On the other hand, the density functional methodologies offer an effective alternative to the conventional correlated methods, due to their significantly lower computational cost[30]. The $^{1}H$ and $^{13}C$ NMR chemical shifts of , 4IPBC, 4IP6MC and 4IP7MC were computed in combination with the B3LYP method from Gauge Atomic Independent Orbital (GAIO) theory using 6-311++G(d, p)/G basis set in vacuum and methanol. The $^{1}H$ and $^{13}C$ NMR shielding values are shown in **Fig. 4** and also the chemical shift values are given in **Table 4**. The chemical shift analysis is one of the most important techniques for the structural analysis for organic compounds[31].

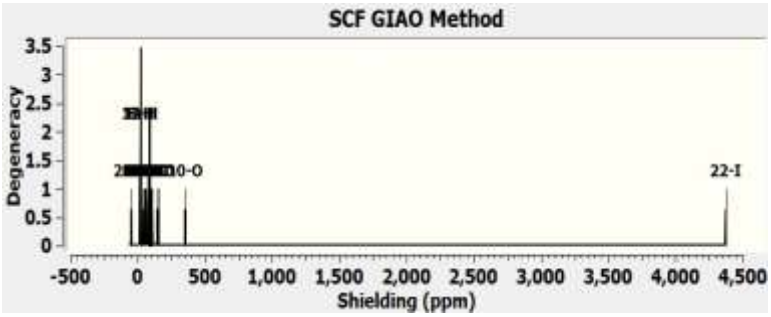


**Fig. 4 NMR spectra of the molecule.**

From observationsin organic molecules, $^{13}C$ NMR chemical shifts are usually lying in the region of 43-158 ppm for and 4IPBC. The $^{1}H$ NMR chemical shifts for atoms 35-H, 33-H, 14-H, 15-H, 28-H, 34-H,

30-H, 8-H, 10-H, 9-H, 29-H, 7-H and 21-H are in the range for vacuum 10-28 ppm. The carbon atoms present in benzene ring, 26-C, 19-C, 4-C, 18-C, 16-C, 24-C, 2-C, 27-C, 5-C, 25-C, 6-C, 3-C, 17-C and 1-C have chemical shifts between 43-99 ppm. The maximum chemical shift for 20-C, 32-C and 13-C. Molecules and 4IPBCboth has maximum shielding value with 13-Cfor methyl group134 ppmand 158 ppm.

**Table 4 NMR shielding values of all biologically active coumarin derivative.**

| Atoms | 4IPBC | Atoms | 4IPBC |
|---|---|---|---|
| 35-H | 10.910 | 26-C | 45.852 |
| 33-H | 12.933 | 19-C | 51.650 |
| 14-H | 17.397 | 4-C | 57.494 |
| 15-H | 18.480 | 18-C | 60.600 |
| 28-H | 18.638 | 16-C | 61.853 |
| 34-H | 22.078 | 24-C | 62.730 |
| 30-H | 25.776 | 2-C | 76.322 |
| 8-H | 26.134 | 27-C | 83.602 |
| 10-H | 26.235 | 5-C | 84.876 |
| 9-H | 26.267 | 25-C | 85.511 |
| 29-H | 26.282 | 6-C | 91.025 |
| 7-H | 26.527 | 3-C | 91.839 |
| 21-H | 27.984 | 17-C | 94.614 |
| | | | |

### 3.4 HOMO-LUMO Surfaces

A molecular orbital is a mathematical function that describes the behavior of an electron or pair of electrons within a molecule. The functions are typically plotted as surface around the molecule structure[32]. The highest occupied molecular orbital (HOMO) and lowest unoccupied molecular orbital (LUMO) may be identified by finding the point where the orbital occupancy changes from occupied to unoccupied. This is often, but not always, the point where the orbital energies change from positive to negative[33,34]. It contains information about both electron transfer (chemical potential) and stability (hardness) and is the better descriptor of global chemical reactivity[35].The computed values of $E_{HOMO}$, $E_{LUMO}$ and corresponding energy gap ($\Delta E$=LUMO-HOMO) of the title molecule in vacuum are -0.33 eV, -0.042 eV, and -0.29eV, respectively. HOMO-LUMO energy diagram is given in **Fig. 5.**

| | | |
|---|---|---|
| **Gas phase** | 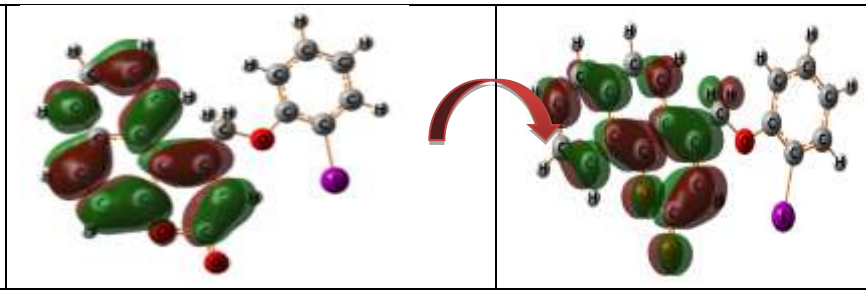 | |

| | | |
|---|---|---|
| **Acetone** | 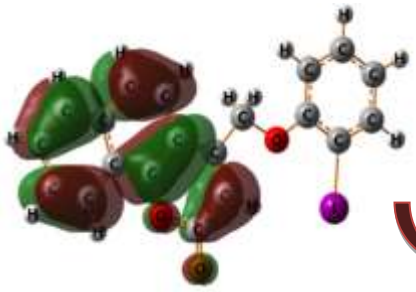 | 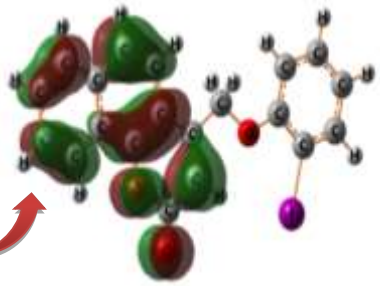 |
| | | |

**Fig. 5 HUMO-LUMO surfaces of 4IPBC in Gas Phase and Acetone.**

### 3.5 Mulliken atomic charges

By default, Gaussian jobs perform a Mulliken population analysis, which partitions the total charge among the atoms in the molecule as shown in **Fig. 6.** Mulliken population analysis is widely used but quite approximate charge distribution scheme which computes charges by dividing orbital overlap evenly between the two atoms involved.. This sort of analysis is commonly used to create input charges for molecular mechanics calculation[36]. In case of and 4IPBC, negative values for2C, 3C, 4C, 5C, 6C, 10O, 11C, 16C 18C, 20C, 23C, 27O, 28O, 29O and 31C. 35I is negative for and positive for 4IPBC. 32H, 23C, 21C is positive for and negative for 21C, 24C 32H, 30H 4IPBC. Positive for 1C, 7H, 8H, 9H, 12H, 13H, 14C, 15C, 17C, 19H, 22H, 25H, 33H and 34H.

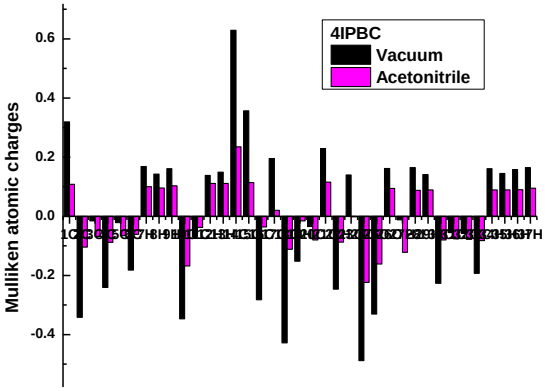


**Fig.6 Mulliken charges of the molecules in Gas phase and acetone.**

### 3.6 ESP and Contor Map

Electrostatic potential is a measure of the potential energy of a proton (or other positive charge) near a molecule and its value differs for different regions within the molecule as shown in **Fig. 7**. Within the resultant display, regions with a high positive and negative electrostatic potential show red and blue, respectively.In the MEP map, red color indicates the electrophilic attack i.e., maximum negative part and blue color indicates the nucleophilic i.e. maximum positive part [38]. In the present map for and 4IPBC, a maximum positive region located around the $CH_2$ group. This group is bonded between coumarin moity and oxygen attached to benzene ring. At the same time, the most negative electrostatic potential area is situated around the C=O bond incoumarin and the second most negative region is present around the oxygen in benzene ring.

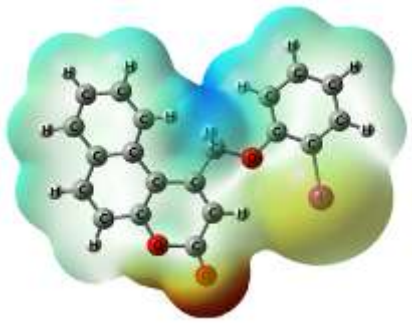

**Fig. 7 ESP of 4IPBC in acetone.**

## 4. Conclusions

Computational studies have been carried out for coumarin derivative 4IPBC using Gaussian 16 software. Semi-empirical method has been used for geometry optimization. The ground state dipole moment estimated from DFT/B3LYP method is greater than excited state dipole moment measured from TD-DFT methodat 6-311++G(d, p)/B3LYP basis set. IR and Raman spectra shows maximum vibrations for C-H, C=O, C-O-C and C=I bonds. $^{13}C$ and $^{1}H$ NMR shielding values have been obtained for GIAO at DFT/B3LYP method at 6-311++G(d, p)/G basis set. Electronic properties like electronegativity, chemical potential, global hardness, global softness and global electrophilicity values were calculated for the molecules in vacuum and solution for TD-DFT method. HOMO-LUMO energy gap for molecule is small, which indicates molecule is soft. ESP map shows electrophilic and nucleophilic sites of the molecule.

**Acknowledgement:**

Authors would like to thank Gaussian software team for introducing Gaussian software to the field of Computational physics and chemistry.

## References

1. B. Shivaleela and S. M. Hanagodimath, “Ground and excited state dipole moments of coumarin derivative 4ATMBC” Conference Proceedings of online International Conference on Advanced Materials, 20th Sep 2020
2. Y. G. Sıdır and I. Sıdır, “Solvent effect on the absorption and fluorescence spectra of 7-acetoxy-6-(2, 3-dibromopropyl)-4, 8-dimethylcoumarin: determination of ground and excited state dipole moments,” *Spectrochim. Acta. A. Mol. Biomol. Spectrosc.*, vol. 102, pp. 286–296, 2013.
3. S. S. Board and N. R. Council, *New worlds, new horizons in astronomy and astrophysics*. National Academies Press, 2011.
4. Shivaleela B, Shivraj G. G, Omnath P. and S. M. Hanagodimath, “Fluorescence quenching of newly synthesized fluorophores in different solvents by bromobenzene using linear Stern-Volmer plots”, Journal of the Maharaja Sayajirao University of Baroda, 55, 1(XIV) (2021) 8-28.
5. M. M. Husain, R. Sindhu, and H. C. Tandon, “Photophysical properties and estimation of ground and excited state dipole moments of 7-diethylamino and 7-diethylamino-4-methyl coumarin dyes from absorption and emission spectra,” *Eur. J. Chem.*, vol. 3, no. 1, Art. no. 1, Mar. 2012, doi: 10.5155/eurjchem.3.1.87-93.519.

6. D. Nagarajaa, N. R. Patilb, R. A. Kusanurc, H. D. Patild, and R. M. Melavankie, "Estimation of Ground and Excited State Dipole Moments of Coumarin Derivatives by Solvatochromic Method," *Int. J. Sci. Res. Publ.*, vol. 2, no. 12, p. 1, 2012.
7. Shivraj G. G, Shivaleela B. and S. M. Hanagodimath, Mass attenuation coefficients, effective atomic number, electron density and kerma of BBPD and BBPO organic molecules, Journal of the Maharaja Sayajirao University of Baroda, 56, 2(I) (2022) 9-18.
8. S. N. Patil, F. M. Sanningannavar, B. S. Navati, N. R. Patil, R. A. Kusanur, and R. M. Melavanki, "Photophysical characteristics of two novel coumarin derivatives: Experimental and theoretical estimation of dipole moments using the solvatochromic shift method," *Can. J. Phys.*, vol. 92, no. 11, pp. 1330–1336, Nov. 2014, doi: 10.1139/cjp-2013-0685.
9. B. Shivaleela and S. M. Hanagodimath, "Studies on molecular structure, UV-visible and HOMO-LUMO analyses of coumarin dye using DFT computational methods," in AIP Conference Proceedings, AIP Publishing, 2021.
10. S. Kumar, "Comparative Study of Excited State Dipole Moment of Coumarin Laser Dyes: Solvent and Substituent Effect," *J Mater Sci Eng B*, vol. 4, pp. 358–365, 2014.
11. Mayadevi K, Raghavendra U. P, Mahantesh B, S. M. Hanagodimath and Tipperudrappa J. Effect of Solvents on Photophysical Properties of Biologically Active Iodinated 4-Aryloxymethyl Coumarin , Journal of Emerging Technologies and Innovative Research, Vol 5, pp. 418-4208, Issue 11, Nov 2018.
12. Mayadevi K, Raghavendra U. P, Mahantesh B, S. M. Hanagodimath and Tipperudrappa J. "Investigation of Polarity Effect of Solvents on Photophysical Properties of Iodinated 4-Aryloxymethyl Coumarin Dye"International Journal of Management, Technology And EngineeringVol. 8, pp 1-8, Issue XII, Dec 2018.
13. S. S. Khemalapure, V. S. Katti, C. S. Hiremath, S. M. Hiremath, M. Basanagouda, and S. B. Radder, "Spectroscopic (FT-IR, FT-Raman, NMR and UV-Vis), ELF, LOL, NBO, and Fukui function investigations on (5-bromo-benzofuran-3-yl)-acetic acid hydrazide (5BBAH): Experimental and theoretical approach," *J. Mol. Struct.*, vol. 1196, pp. 280–290, Nov. 2019, doi: 10.1016/j.molstruc.2019.06.078.
14. S. M. Hiremath *et al.*, "Molecular structure, vibrational spectra, NMR, UV, NBO, NLO, HOMO-LUMO and molecular docking of 2-(4, 6-dimethyl-1-benzofuran-3-yl) acetic acid (2DBAA): Experimental and theoretical approach," *J. Mol. Struct.*, vol. 1171, pp. 362–374, Nov. 2018, doi: 10.1016/j.molstruc.2018.05.109.
15. C. G. Renuka, K. Shivashankar, P. Boregowda, S. S. Bellad, M. V. Muregendrappa, and Y. F. Nadaf, "An Experimental and Computational Study of 2-(3-Oxo-3H-benzo[f] chromen-1-ylmethoxy)-Benzoic Acid Methyl Ester," *J. Solut. Chem.*, vol. 46, no. 8, pp. 1535–1555, Aug. 2017, doi: 10.1007/s10953-017-0661-4.
16. İ. Sıdır and Y. G. Sıdır, "Solvatochromism and intramolecular hydrogen-bonding assisted dipole moment of phenyl 1-hydroxy-2-naphthoate in the ground and excited states," *J. Mol. Liq.*, vol. 221, pp. 972–985, 2016.
17. A. K. Mishra and S. P. Tewari, "Density functional theory approach towards bioactivity analysis of Isovallesiachotamine natural bio molecule," *Int J Sci. Res. Phys. Appl. Sci.*, pp. 118–131, 2019.
18. M. ea Frisch *et al.*, "Gaussian 16, revision C. 01." Gaussian, Inc., Wallingford CT, 2016.

19. R. A. Gaussian09, "1, mj frisch, gw trucks, hb schlegel, ge scuseria, ma robb, jr cheeseman, g. Scalmani, v. Barone, b. Mennucci, ga petersson et al., gaussian," *Inc Wallingford CT*, vol. 121, pp. 150–166, 2009.
20. B. Siddlingeshwar and S. M. Hanagodimath, "Estimation of the ground and the first excited singlet-state dipole moments of 1,4-disubstituted anthraquinone dyes by the solvatochromic method," *Spectrochim. Acta. A. Mol. Biomol. Spectrosc.*, vol. 75, no. 4, pp. 1203–1210, Apr. 2010, doi: 10.1016/j.saa.2009.12.007.
21. G. B. Mathapati, P. K. Ingalgondi, P. Omnath, B. Shivaleela, G. G. Shivraj, and S. M. Hanagodimath, "Estimation of ground and excited state dipole moments of newly synthesized coumarin molecule by Solvatochromic shift method and Gaussian software," *Int. J. Sci. Res. Phys. Appl. Sci.*, vol. 7, pp. 38–43, 2019.
22. Shivaleela B and S M Hanagodimath, "Quantum Chemical Calculations on NBO, NLO, Spectroscopic (UV-Visible, IR, Raman, 1H and 13C NMR) Analysis, HOMO-LUMO and ESP Map of Fluorescent Molecule by Semi-Empirical and Hartree-Fock Optimization Methods."Journal of International Academy of Physical Sciences, Vol 27, 1(2023), 69-78.
23. K. Carthigayan, S. Xavier, and S. Periandy, "HOMO–LUMO, UV, NLO, NMR and vibrational analysis of 3-methyl-1-phenylpyrazole using FT-IR, FT-RAMAN FT-NMR spectra and HF-DFT computational methods," *Spectrochim. Acta. A. Mol. Biomol. Spectrosc.*, vol. 142, pp. 350–363, May 2015, doi: 10.1016/j.saa.2015.02.035.
24. S. Kumar, V. C. Rao, and R. C. Rastogi, "Excited-state dipole moments of some hydroxycoumarin dyes using an efficient solvatochromic method based on the solvent polarity parameter, ETN," *Spectrochim. Acta. A. Mol. Biomol. Spectrosc.*, vol. 57, no. 1, pp. 41–47, Jan. 2001, doi: 10.1016/S1386-1425(00)00330-9.
25. İ. Sıdır, Y. G. Sıdır, H. Berber, and F. Demiray, "Emerging ground and excited state dipole moments and external electric field effect on electronic structure. A solvatochromism and theoretical study on 2-((phenylimino)methyl)phenol derivatives," J. Mol. Liq., vol. 206, pp. 56–67, Jun. 2015, doi: 10.1016/j.molliq.2015.01.056.
26. Shivaleela B, Shivraj G. G. and S. M. Hanagodimath, "Estimation of Dipole Moments by Solvatochromic Shift Method, Spectroscopic Analysis of UV-Visible, HOMO-LUMO, ESP Map, Mulliken Charges, NBO And NLO Properties of Benzofuran Derivative" Results in Chemistry, Vol 6, Dec 2023, 101046. https://doi.org/10.1016/j.rechem.2023.101046
27. S. M. Hiremath, "Vibrational, electronic and reactivity insight on (5-chloro-benzofuran-3-yl)-acetic acid hydrazide: A Spectroscopic and DFT approach," *J. Mol. Struct.*, vol. 1239, p. 130479, Sep. 2021, doi: 10.1016/j.molstruc.2021.130479.
28. S. G. Gounhalli, S. Basavaraj, and S. M. Hanagodimath, "Spectroscopic Analysis of NMR, IR, Raman and UV-Visible, HOMO-LUMO, ESP And Mulliken Charges of Coumarin Derivative by Density Functional Theory," *J. Maharaja Sayajirao Univ. Baroda*, 55, 1 (XIV) (2021) 213-229.
29. A. Eşme and S. G. Sağdınç, "Spectroscopic (FT–IR, FT–Raman, UV–Vis) analysis, conformational, HOMO-LUMO, NBO and NLO calculations on monomeric and dimeric structures of 4–pyridazinecarboxylic acid by HF and DFT methods," *J. Mol. Struct.*, vol. 1147, pp. 322–334, 2017.
30. S. M. Hiremath, S. S. Khemalapure, C. S. Hiremath, A. S. Patil, and M. Basanagouda, "Quantum chemical computational and spectroscopic (IR, Raman, NMR, and UV) studies on the 5-(5-methoxy-

benzofuran-3-ylmethyl)-3H-[1, 3, 4] oxadiazole-2-thione," *J. Mol. Struct.*, vol. 1210, p. 128041, Jun. 2020, doi: 10.1016/j.molstruc.2020.128041.

31. S. G. Gounhalli, S. Basavaraj, and S. M. Hanagodimath, "Comparative Study of NMR, IR, Raman Spectroscopy, HOMO-LUMO Surfaces of Benzofuran and Coumarin Derivative in Vacuum and Methanol," *J. Maharaja Sayajirao Univ. Baroda Issn*, vol. 56, 2(I) (2022) 169-186.
32. Shivaleela B, Shivraj G. G, Omnath P. and S. M. Hanagodimath, "Quenching of fluorescence, dipole moments and DFT studies of newly synthesized amino-thiadiazole coumarin derivative" Journal of the Maharaja Sayajirao University of Baroda, 55, 1 (XIV) (2021) 200-220.
33. V. Balachandran, V. Karpagam, B. Revathi, M. Kavimani, and G. Ilango, "Conformational stability, spectroscopic and computational studies, HOMO–LUMO, NBO, ESP analysis, thermodynamic parameters of natural bioactive compound with anticancer potential of 2-(hydroxymethyl) anthraquinone," *Spectrochim. Acta. A. Mol. Biomol. Spectrosc.*, vol. 150, pp. 631–640, 2015.
34. B. Shivaleela and S. M. Hanagodimath, "UV-Visible spectra, HOMO-LUMO studies on coumarin derivative using Gaussian software" Conference Proceedings of one day online International Conference on Advanced Materials, 20th Sep 2020.
35. S. M. Hiremath *et al.*, "Structural, spectroscopic characterization of 2-(5-methyl-1-benzofuran-3-yl) acetic acid in monomer, dimer and identification of specific reactive, drug likeness properties: Experimental and computational study," *J. Mol. Struct.*, vol. 1178, pp. 1–17, Feb. 2019, doi: 10.1016/j.molstruc.2018.10.007.
36. M. K. Priya, B. K. Revathi, V. Renuka, S. Sathya, and P. S. Asirvatham, "Molecular structure, spectroscopic (FT-IR, FT-Raman, 13C and 1H NMR) analysis, HOMO-LUMO energies, Mulliken, MEP and thermal properties of new chalcone derivative by DFT calculation," *Mater. Today Proc.*, vol. 8, pp. 37–46, 2019.
37. M. Arivazhagan and J. S. Kumar, "Vibrational assignment, HOMO–LUMO, first-hyperpolarizability and Mulliken's charge analysis of 2, 7-dinitrofluorene," 2012.
38. A. H. Radhi *et al.*, "HOMO-LUMO energies and geometrical structures effecton corrosion inhibition for organic compounds predict by DFT and PM3 methods," *NeuroQuantology*, vol. 18, no. 1, p. 37, 2020.